

<sup>1</sup> Universitat Politècnica de Catalunya, Dept. Matemàtica Aplicada I, Barcelona, Spain

<sup>2</sup> Centro Meteorológico de Cienfuegos, Cienfuegos, Cuba

<sup>3</sup> Grupo de Climatología, Universidad de Barcelona, Barcelona, Spain

## Objective synoptic classification combined with high resolution meteorological models for wind mesoscale studies

C. Soriano<sup>1</sup>, A. Fernández<sup>2</sup>, and J. Martin-Vide<sup>3</sup>

With 9 Figures

Received June 29, 2004; revised September 27, 2004; accepted January 10, 2005

Published online: September 15, 2005 © Springer-Verlag 2005

### Summary

A methodology developed for automatic classification of Objective Synoptic Processes (OSP) and its application to the study of the mesoscale atmospheric circulatory patterns associated with them is described. The classification was based on the analysis of the evolution of surface pressure and geopotential height at 500 hPa during three days. An iterative procedure results in an objective grouping of the main configurations describing different large-scale situations. This routine has been applied over an appropriate domain covering the Iberian Peninsula to obtain OSPs in the region for the two month period July–August, using daily synoptic maps for years 1990 to 1999 (a total of 7304 surface and 500 hPa synoptic maps have been used in the analysis). Finally, for a characteristic day for two of the OSPs obtained, a mesoscale meteorological model (TAPM) has been run at high resolution for the region of Catalonia, Northeastern Spain, in order to describe the local atmospheric circulatory patterns associated with a given large-scale situation. Results show that the complex orography modifies the large-scale forcings resulting in wind fields with a very important horizontal variability, significant daily cycle, and specific local features related to orographic elements, which the model was able to incorporate due to the highly-resolved orography used.

### 1. Introduction

It is a well know fact that local topography in a region is a key factor in the establishment of the

air fluxes in the mesoscale under a given synoptic situation. Synoptic forcings are adapted to the particular orographic characteristics, resulting in wind fields with very specific local features (for instance, Stull, 1988). However, synoptic analysis constitutes the frame under which local circulations are developed. Similar synoptic situations generally lead to similar local scale wind patterns and that is the reason why it is useful to have a good classification of these synoptic processes in order to be able to identify the local winds associated with each of them.

The Iberian Peninsula, the geographical framework under which this work has been carried out, has a remarkable geographical complexity, due to its important orography (wide range of altitudes, 0–3400 m) and its location in southwestern Europe (at mid-latitude, but under the influence of air masses with different origins ranging from polar to subtropical). This fact leads to an important atmospheric complexity in the region, where pressure fields are not always clearly defined and are not always well connected with those at higher levels, especially in summertime.

The most commonly used catalogues of synoptic classifications for the Iberian Peninsula are those of Linés (1981) with 25 types defined

based on 300 hPa maps, Font Tullot (1983) with 23 types combining surface pressure and 500 hPa, Martín-Vide (1991) with 16 types using the same levels for classification, and Capel Molina (2000) with 18 types of synoptic classifications based on surface pressure and 500 or 300 hPa maps. All of these are based on subjective methods of classification.

In the last few years, several authors have published automated classification schemes for the Iberian region, most of which are connected to some specific climate application. Two main currents can be identified in these works. The first group is based on the seminal work of Jenkinson and Collison (1977), and is illustrated in the papers of Goodess and Palutikof (1998), Trigo and DaCamara (2000), Spellman (2000), Goodess and Jones (2002), Martín-Vide (2002) and Rasilla (2003). The second group of works is based on the use of multivariate methods (more specifically, principal component analysis, PCA) followed by cluster analysis, such as those of Galán (1989), Zhang et al (1997), Corte-Real et al (1998; 1999), Romero et al (1999a; 1999b) and Esteban et al (2005). There are other studies of this issue, but they cover the whole Mediterranean area (Düneloh and Jacobeit, 2003). Most of them apply the classification schemes to study the relationship between the synoptic situation and precipitation variability (a variable of special concern in the Iberian Peninsula due to its relatively scarce pluviometry).

For the present study, Goodess and Palutikof (1998), Corte-Real et al (1999) and Trigo and DaCamara (2000) have been particularly useful. Goodess and Palutikof (1998) detected eight circulation types related to the development of daily rainfall scenarios for SE Spain.: Cyclonic, hybrid-cyclonic, unclassified/light flow-cyclonic, anticyclonic/hybrid-anticyclonic, unclassified/light flow-anticyclonic, W/NW/SW/N directional type, E/NE directional type and S/SE directional type. Corte-Real et al (1999) established four circulation patterns for daily precipitation in Portugal: blocking-like, summer dry, winter dry and rainy. Finally, Trigo and DaCamara (2000) described ten weather types for the precipitation regime in Portugal: anticyclonic, cyclonic and the usual eight directional types. The new classification obtained with the methodology described

in this contribution has been compared with the types described in these references.

We propose and apply a new objective classification method for synoptic situations (obtained by using statistical methods) that is dynamic (taking into consideration the situation during the previous and posterior day to the day studied). The types of situations obtained with this multivariate analysis at two levels (Surface Pressure, Psfc, and 500 hPa geopotential height, Z500) are what we call Objective Synoptic Processes (OSPs). The method considers three day groups (corresponding to days  $D - 1$ ,  $D$  and  $D + 1$ ) and is based on the minimization, by means of iterative tools, of the distance among the groups. Although using a different method, there exists some previous works of synoptic classifications using groups of three days (Bardossy and Plate, 1992; Shubert, 1994). The final result consists of average pressure and geopotential maps for each of the Objective Synoptic Processes identified with the algorithm.

The next step, and regarding the application of this classification to investigate local/mesoscale atmospheric circulations, is executing a mesoscale meteorological model at high resolution ( $2 \times 2 \text{ km}^2$ ) for the region of Catalonia (Spain), that is characterized by a very complex orography next to the Mediterranean Sea. The model has been run, for this application, for a characteristic day belonging to some of the OSPs identified with the procedure. More precisely, the atmospheric circulatory patterns associated with two of these OSPs have been described.

## 2. Objective synoptic processes: methodology

Calculation of the OSPs for the period 1990–1999 is based on the methodology proposed by Fernández and Díaz (in press) and Fernández et al (2003). OSPs were found for the two month period July–August. The procedure follows the steps described below:

- (a) Calculation of the iterations between groups of three consecutive synoptic situations, evaluating the distance between the groups, which is given by the general formula:

$$\text{Dist}(k) = \left( \sum_{i=1,m} \sum_{j=1,n} |F_{\text{mod}}(i, j, k) - F_{\text{dat}}(i, j, k)| \right) / m * n,$$

where  $F_{\text{mod}}(i, j, k)$  is the array containing the data for each iteration for the variables used (that is,  $P_{\text{sf}}c$  or  $Z500$ ), and  $F_{\text{dat}}(i, j, k)$  is daily data included for the extraction of the OSPs. Index  $i$  corresponds to rows (latitude) and index  $j$  corresponds to columns (longitude) in the arrays containing the data of  $P_{\text{sf}}c$  and  $Z500$ . Index  $k$  accounts for the number of iterations for each OSP. The total number of rows of the arrays is  $m$  and the total number of columns is  $n$ .

- (b) Iterative process for the calculation of the distances, with a statistical significance level  $\alpha \leq 0.05$ . Determination of the group of iterations  $\text{Dist}(k)$  for which condition (a) is fulfilled. Calculation of  $S_1$  and  $S_2$  in the discriminant formula of Miller for the selection of optimized groups comprising an OSP.

$$S_1(x_p) = \sum_{g=1,G} \sum_{k=1,n_g} (x_{\text{pgk}} - x_{\text{pg}})^2,$$

$$S_2(x_p) = \sum_{g=1,G} n_g (x_{\text{pg}} - x_p)^2,$$

where  $(x_{\text{pgk}} - x_{\text{pg}})^2$  represents the squared differences between the average of each OSP group and each of the observed  $P_{\text{sf}}c$  and  $Z500$  values.  $G$  represents the total number of OSPs.  $S_1(x_p)$  accounts for the sum, for all the OSPs, of the total deviation within all the groups. The term  $(x_{\text{pg}} - x_p)^2$  represents all the squared differences between the average for every OSP and the average for the whole sample under analysis, weighted with the number of cases for each OSP. Finally,  $S_2(x_p)$  gives information of the differences between the different groups.

- (c) Calculation of the quotient  $S_2(x_p)/S_1(x_p)$  for all the iterations calculated, selecting the one which maximizes this quantity, thereby establishing the groups that form the OSPs.
- (d) Extraction of the averaged fields for  $P_{\text{sf}}c$  and  $Z500$  for days  $D - 1$ ,  $D$  and  $D + 1$ , the group of three days constituting each OSP. Calculation of the relative frequency of occurrence for each OSP during the studied bi-month. The particular days belonging to each group are identified.

Not all the cases that are analyzed are classified into one of the OSPs. Those groups of three days that fail to belong to any of the OSPs correspond to very particular and infrequent meteorological situations and are disregarded in the further anal-

ysis, just as those OSP that have a frequency less than 1%.

### 3. Application to the Iberian Peninsula: OSPs obtained for July–August

The methodology described above has been applied to July–August for the period 1990–1999. The restriction of the two-month period has to do with the important seasonal variability of the atmospheric situations for this region. For example, some of the situations, such as the barometric swamp followed by the formation of a thermal low (studied here), only occur during summertime (the well described Iberian Thermal Low, Millán et al, 1997). Besides, summertime is an interesting season to test this new classification method. The weak relationship between large-scale circulation modes and regional climate during this time of the year has often lead to unclassified situations in the existing classifications. The new methodology can help to classify these cases with low surface pressure gradients.

The domain for the calculations was chosen by taking into account that it must guarantee a successful automatic classification. On the one hand, the domain had to be big enough to cover a wide planetary region in order to identify the synoptic structures that are involved in the classification. On the other hand, it had to have at a resolution high enough to keep the information of atmospheric structures in the meso- $\alpha$  (typical size of the order of 1000 km and time scales of one day) and meso- $\beta$  scales (typical size of the order of a few 100-km and time scales of a few hours), which play an important role in the region we are studying, and lead to very different atmospheric situations.

Following these constraints, the domain chosen consisted of 17 latitudinal cells and 25 longitudinal cells (a total of 425 grid points), at a resolution of 2.5 degrees. The working window covered 25° N–65° N and 30° W–30° E. The variables used in the classification are surface pressure and geopotential height at 500 hPa, extracted from the reanalysis maps of the National Center for Atmospheric Research NCEP-NCAR for period 1990–1999 (Kalnay et al, 1996).

The selection of the OSPs for July–August 1990–1999 led to 22 different types of synoptic

**Table 1.** Number of cases, relative frequency and return period for each OSP, for July–August (period 1990–1999)

OSP	No. of cases	Frequency (%)	Return period (days)
1	73	11.8	8.5
2	59	9.5	10.5
3	52	8.4	11.9
4	43	6.9	14.5
5	38	6.1	16.4
6	38	6.1	16.4
7	35	5.6	17.9
8	28	4.5	22.2
9	28	4.5	22.2
10	27	4.4	22.7
11	24	3.9	25.6
12	22	3.5	28.6
13	21	3.4	29.4
14	18	2.9	34.5
15	18	2.9	34.5
16	17	2.7	37.0
17	14	2.3	43.5
18	13	2.1	47.6
19	9	1.5	66.7
20	8	1.3	76.9
21	8	1.3	76.9
22	8	1.3	76.9

situations. Table 1 shows the classification obtained, with the corresponding frequency and return period for each case. Figure 1 shows the representation of the average Psfc and Z500 for the first 10 OSPs. Images include maps for the three days describing each situation.

The classification resulted in what at first seems to be a high number of OSPs, especially considering that the analyzed period corresponds to summertime, a time of the year with little surface pressure gradient. This fact can be explained if we take into account that the classificatory process uses groups of three days ( $D - 1$ ,  $D$  and  $D + 1$ ) and is conducted at two levels (SFC and Z500). Therefore, there are days which might seem similar in their central day, but show differences in their respective previous/following days or surface/height fields, resulting in being classified into different OSPs.

The most frequent OSP (OSP1) occurs 11.8% of the days studied, while OSP22 (the less frequent), occurs only 1.3% of the days. Decrease of the frequency is almost exponential. The top six OSPs comprise almost half the days analyzed (48.8%), and the first 12 account for 75%. As for the return period, this follows an inverse

evolution, with probability for OSP1 being of seven times in the two month (return period of 8.6 days), while OSP22 only occurs once every 1.3 years (return period of 76.9 days).

Table 2 summarizes the main synoptic characteristics of the first ten OSPs. It shows the prevalence of westerly flows at 500 hPa (SW to NW), with weak zonal indices for six types (three of them showing a typical blocking pattern configuration), and strong zonal index only for one OSP. At the surface, eight types show the typical configuration consisting of a trough starting over the Saharan desert with the axis directed towards the center of the Iberian Peninsula. The weak surface pressure gradient has not allowed the identification of clear synoptic flow over Catalonia for four of these ten OSPs.

Also in Table 2, the first ten OSPs are associated with some of the circulation and weather types proposed by Goodess and Palutikof (1998), Corte-Real et al (1999), and Trigo and DaCamara (2000). The S/SE directional type described for the SE Iberian Peninsula in the first mentioned work can be found in three OSPs. The summer dry and blocking pattern types of the second work have been identified in eight OSPs. Finally, NE and NW types in Portugal from the third work were found in six OSPs.

Certain traits between the synoptic situation and the mesoscale wind pattern have been analyzed only for two of the OSPs identified by the methodology: OSP6 and OSP5. This selection is based on the relatively high frequency of their occurrence (about 6% of the total cases for both of them) and also because they are very different from the synoptic point of view. This last fact assured that the results from the mesoscale simulation would be different enough and would therefore illustrate the usefulness of the proposed methodology to obtain a good classification of the synoptic situations and the accompanying local wind patterns.

The next sections in this contribution describe the two OSPs under consideration, and the specific days from the studied period which have been classified as belonging to them. These two days are the ones that, for the moment, have been simulated with the mesoscale meteorological model.

In order to demonstrate the robustness of this method, for one of the OSP, two different days have been simulated, in order to ascertain the similarity of the regional circulatory patterns for each day.

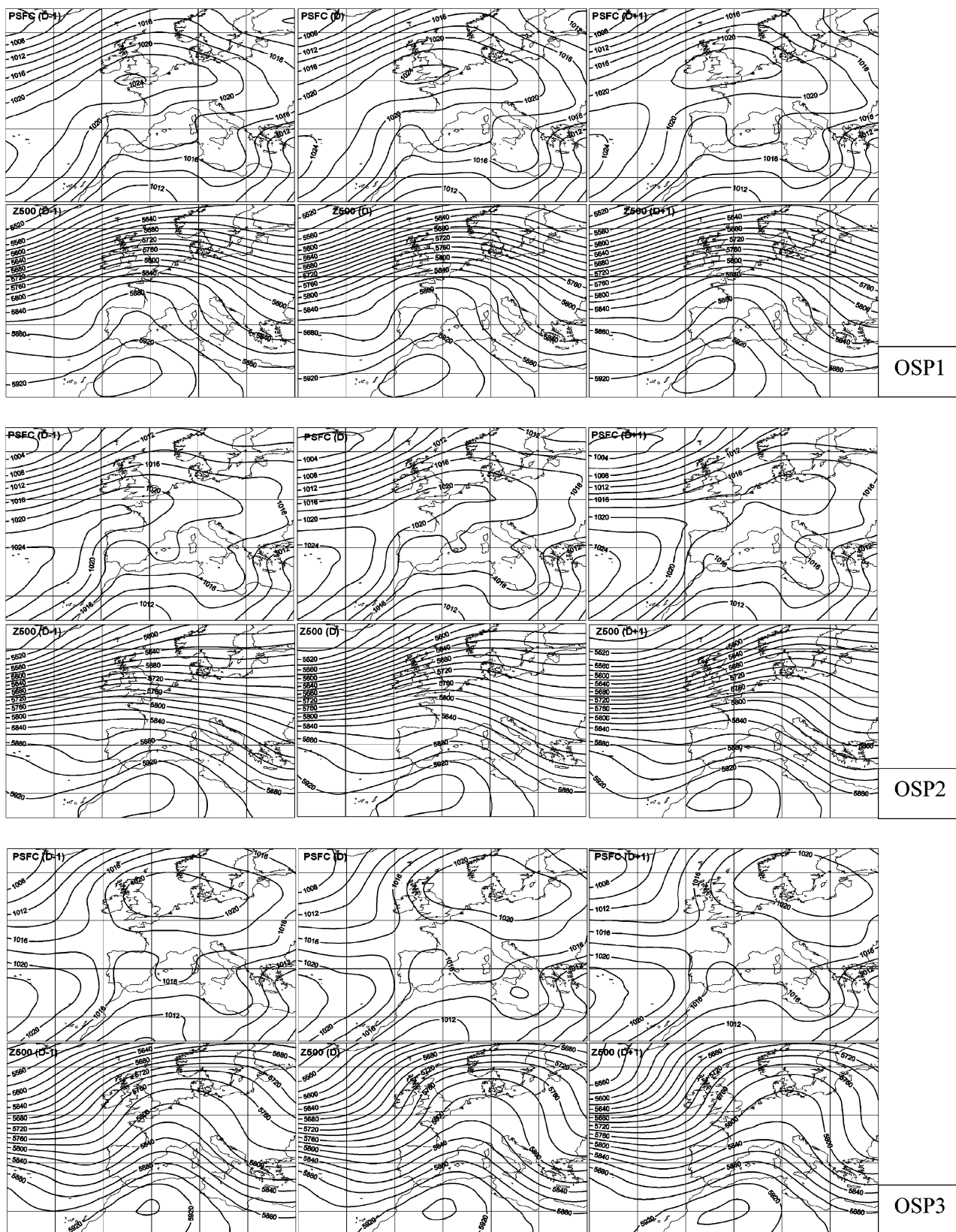


Fig. 1. Synoptic maps for the first ten OSPs obtained with the new classification method. For each OSP, Pscf and Z500 have been represented for days D - 1, D and D + 1

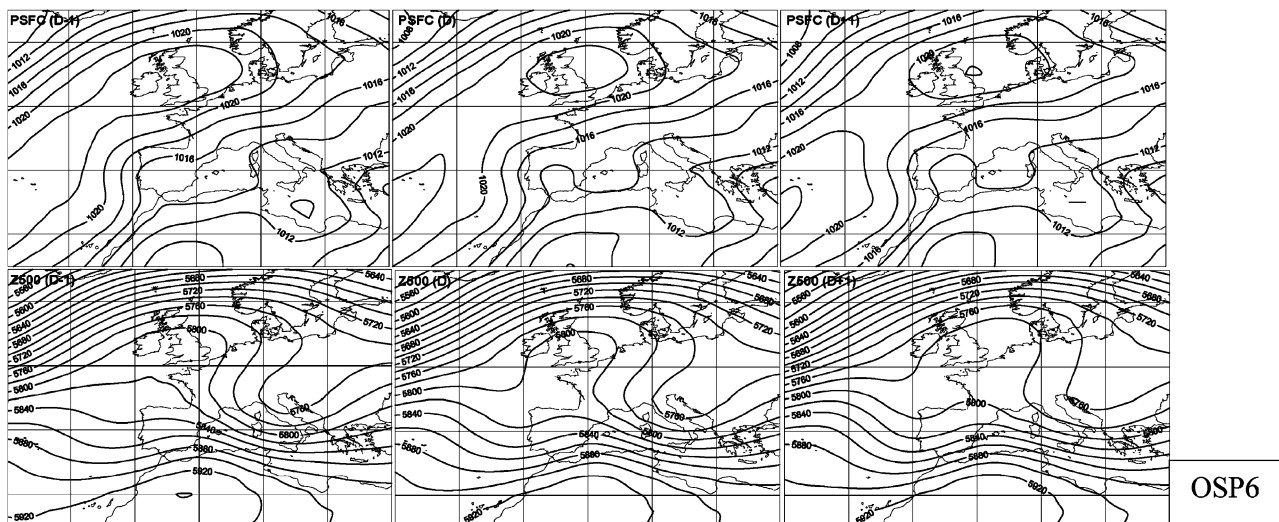
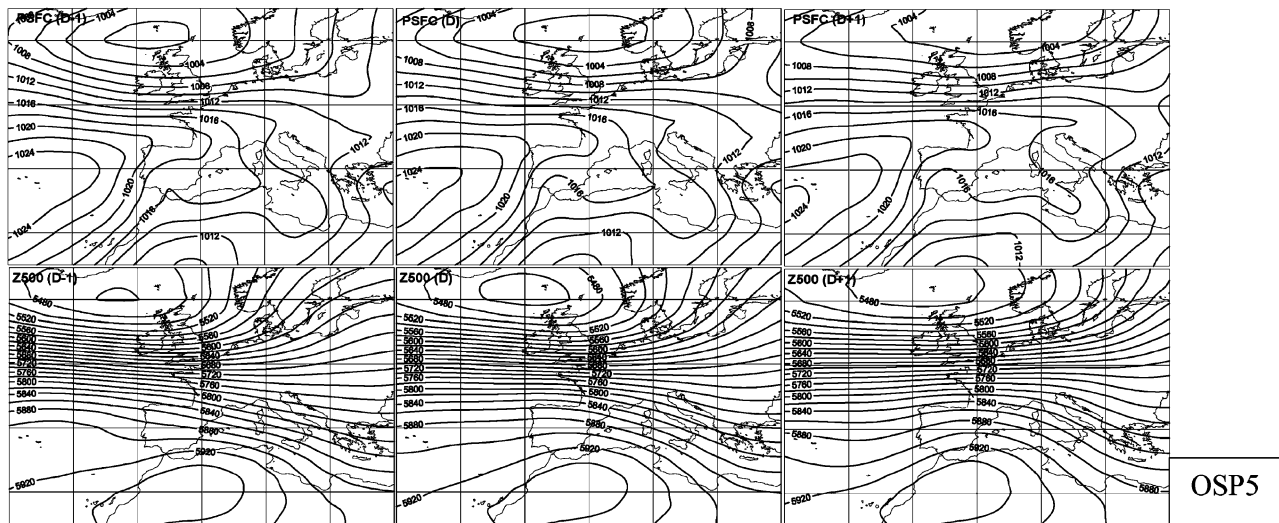
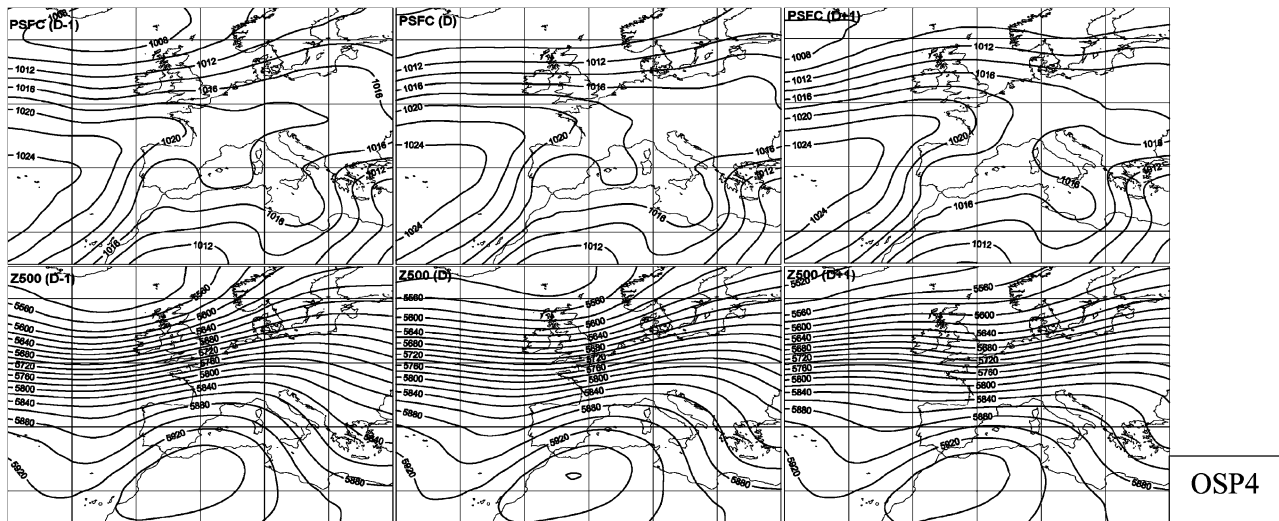


Fig. 1 (continued)

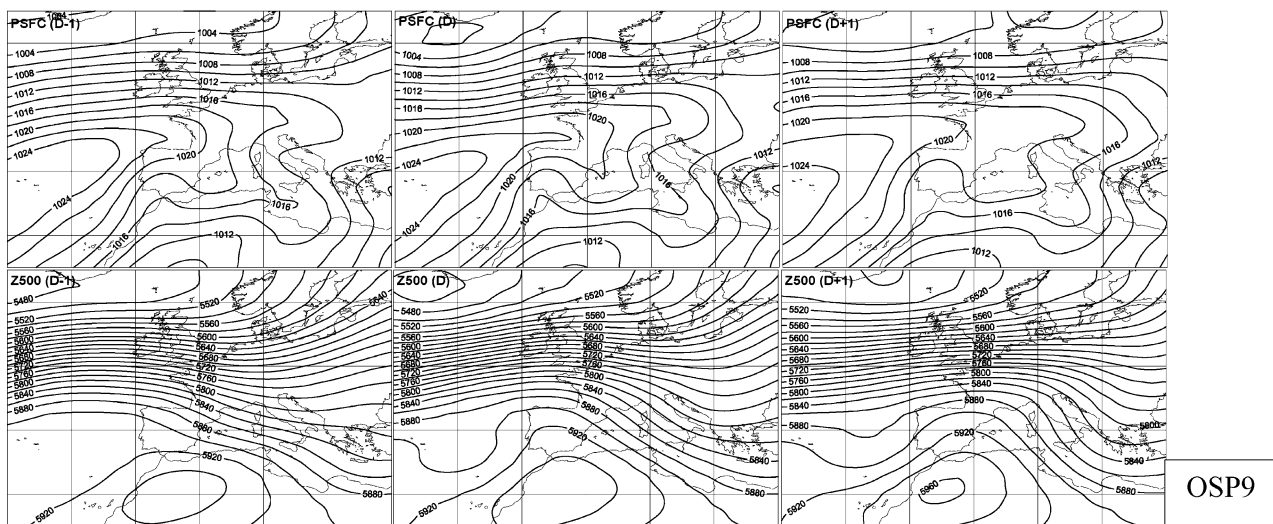
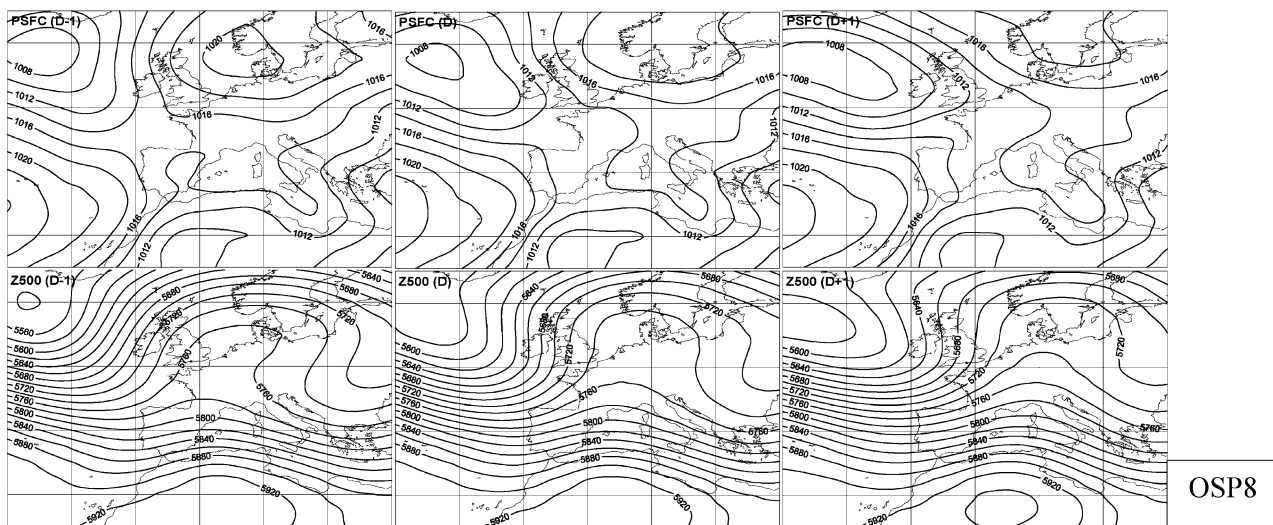
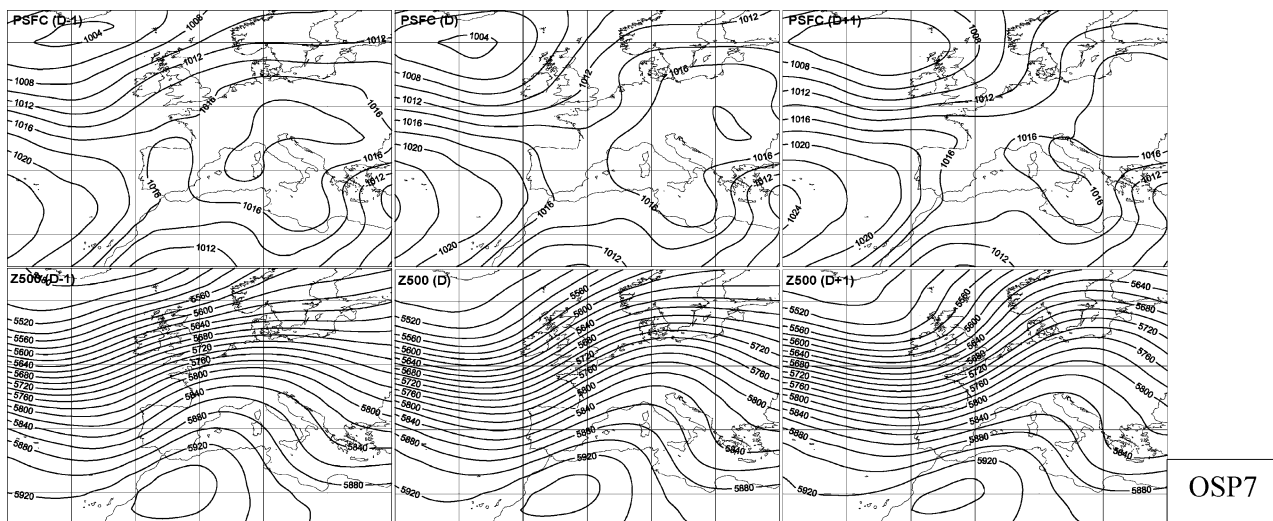


Fig. 1 (continued)

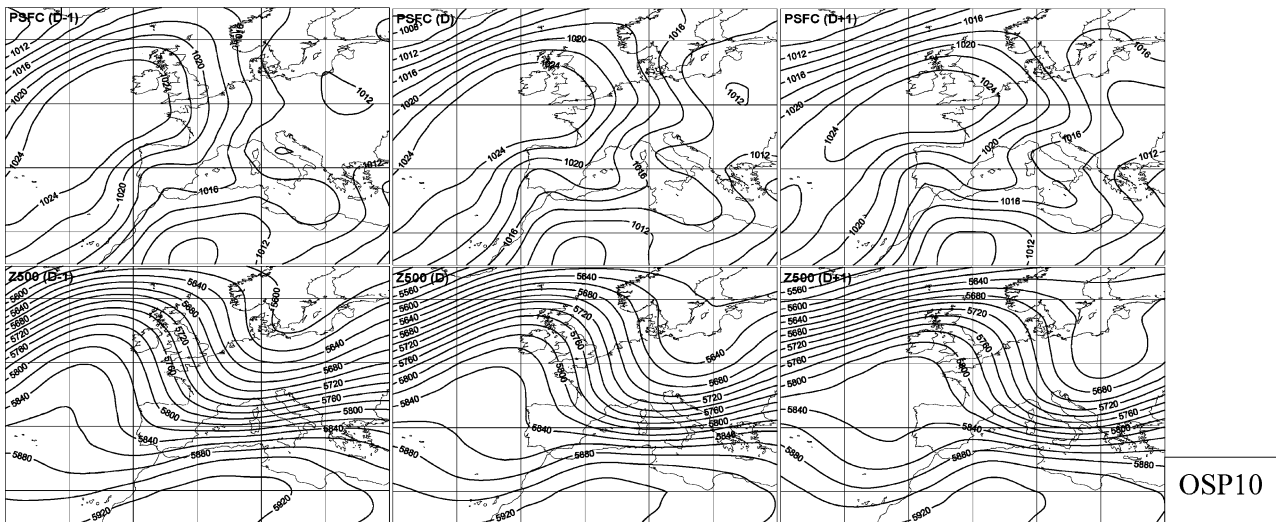


Fig. 1 (continued)

### 3.1 Analysis of OSP6: July 10, 1999

The synoptic situation under OSP6, whose Psfc and Z500 representation for days D – 1, D and D + 1 can be found in Fig. 1, has many similarities with that during July 10, 1999 (Psf and Z500 are shown in Fig. 2 but only for the central day).

The most important element identified from the surface map is the North Atlantic Anticyclone over the British Islands and the North Sea, with a centre isobar of 1032 hPa, resulting in an easterly–northeasterly flow over northern France and the Cantabric Sea. Most of the Iberian Peninsula and the Mediterranean Basin showed a very low pressure gradient, and the situation can be qualified as “Barometric Swamp”.

As for the map at 500 hPa, an anticyclonic wave was located over the North Atlantic and the British Islands (corresponding to a typical blocking pattern) and a trough was present over Central Europe and Italy. The disconnection between surface and high altitude allows us to describe this cold depression as a cold pool. Northwest Africa is under the influence of an anticyclone. This configuration is similar in the OSP6 average Z500 map, although the cold pool is not completely closed and is only represented as a trough.

### 3.2 Analysis of OSP5: July 14, 1999

In the surface maps (Fig. 3) a tight group of isobars with western and northwestern orientation was located in the North Atlantic, with a depres-

sion north of the British Islands. The Iberian Peninsula was under the influence of a northwesterly flow. Low pressures over Africa extend towards Spain as a trough. The configuration in the OSP5 average maps is similar.

Analysis map at height shows a high index circulation, with isohypses in a zonal disposition with high gradient, over the North Atlantic and Western Europe. A depression was positioned to the west of Morocco, while a wide anticyclone was situated over Northern Africa. Also in this case the agreement with OSP5 Z500 map is noticeable.

## 4. The mesoscale meteorological model TAPM: description and application to the study region

The next step in this study has been the simulation, with a high resolution mesoscale model, of a representative day of the OSPs analyzed above. The model chosen was TAPM (The Air Pollution Model), developed by the Atmospheric Research Group of CSIRO (*Commonwealth Scientific and Industrial Research Organization*), in Australia (Hurley et al, 2001; Hurley, 2002). TAPM is a complete modeling system for the study of atmospheric transport, although only the meteorological module is used in the current study. It is a non-hydrostatic and full primitive-equation model with an  $E - \varepsilon$  turbulence scheme (that is, its closure scheme has a prognostic equation for the turbulence kinetic energy and its dissipation). It works with vertical terrain-following

**Table 2.** Main synoptic characteristics of the 10 first OSPs and corresponding types in Goodess and Palutikof (1998) (GP), Corte-Real et al (1999) (C-R et al), and Trigo and DaCamara (TD) (2000)

OSP	500 hPa			Sea level (D-day)				Type		
	Zonal index	Blocking pattern	D-day flow direction over Catalonia	Anticyclone localization	Main low localization	Sahara-Iberia trough	Synoptic flow direction in Catalonia	GP	C-R et al	TD
1	Weak		NW	British Isles Azores	SW Iceland	✓	E		Blocking	NE
2	Moderate		W	Azores	SW Iceland	✓	Undeterm.		Summer dry	NE
3	Weak	✓	SW	Azores and North Sea-Scandinavia Azores	SW Iceland	✓	SE		Blocking	
4	Moderate		SW	Azores	N Europe	✓	Undeterm.		Summer dry	NE
5	Strong		W-NW	Azores	N North Sea	✓	N	S/SE	Summer dry	
6	Weak	✓	NW	British Isles Azores and Centreurope Azores and Scandinavia Azores	SW Iceland	✓	Weak NE		Blocking	NE
7	Weak		SW	Azores and Centreurope Azores and Scandinavia Azores	S Iceland		Undeterm.		Rainy	NW
8	Weak	✓	SW	Azores and Scandinavia Azores	S Iceland		Undeterm.		Rainy	NW
9	Moderate		NW	Azores	S Iceland	✓	N	S/SE	Summer dry	
10	Weak		NW-N	British Isles-Azores	SW Iceland	✓	N-NE	S/SE	Summer dry	E

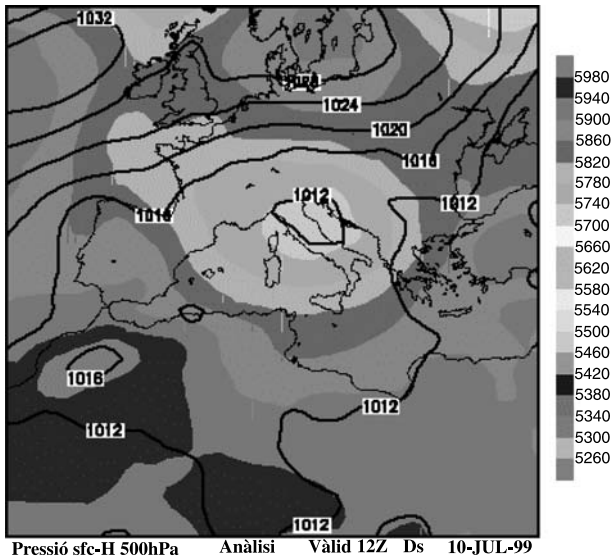


**Fig. 2.** Synoptic map at 12 UTC for July 10, 1999 (Psfc with black isolines and Z500 shaded)

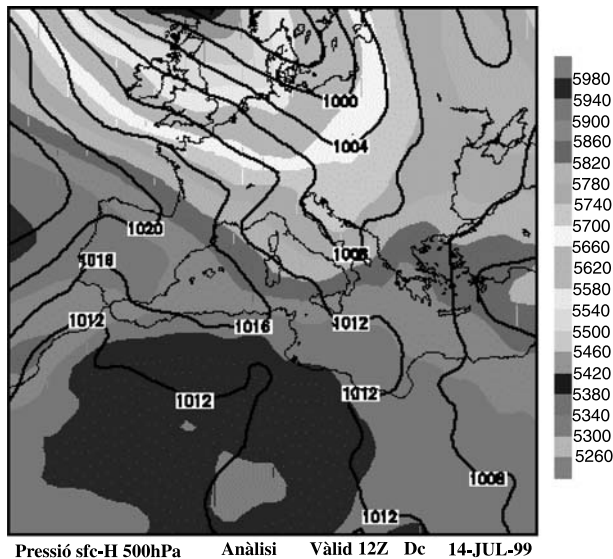


**Fig. 3.** Synoptic map at 12 UTC for July 14, 1999 (Psfc with black isolines and Z500 shaded)

coordinates (sigma-level, to incorporate the topography smoothly into the model, by normalizing the vertical coordinate by the fluid’s depth) and non-staggered grids (where the mesh points are not shifted with respect to each other by half an interval) are used in the numerical solution of TAPM’s equations. It uses topography and land-use data (from the US Geological Service database) in order to characterize with detail the terrain and its parameters interacting with the atmosphere.

The model needs input data from a large-area model that will be used for initialization and boundary conditions. For this case, initialization and boundary conditions (every 6 hours) have been obtained from the analysis of the Australian Bureau of Meteorology global analysis model (Puri et al, 1998; Hart, 1998). To allow a better transference of this synoptic information to the local scale, TAPM allows nesting techniques in order to account for larger-scale flows in the inner grids. This is how wind fields simulated at high resolution over a domain covering a small region can include effects introduced by orographic features not contained within this inner domain, but important to the establishment of the circulatory pattern in the regional scale.

In the present study, four nested domains have been used, each of them consisting of  $150 \times 150$  cells in the horizontal dimensions and 30 vertical levels. The horizontal resolution of each of the domains was 20, 10, 4 and 2 km, with the inner of the domains covering the whole Catalan region. Figure 4 shows the area covered by the domains and its main topographical features, displaying the complexity of the orography in the study area. The most important element is the Pyrenees, a mountainous barrier between Spain and France with maximum heights over 3000 m. The Mediterranean Sea will also play an important role in the establishment of the local circulations due to differential heating between land and sea. Finally, looking more closely to the inner domain (Fig. 4d), where the results of the mesoscale model will be analyzed, the presence of two river valleys, of the Llobregat river (in the central coast) and the Ebro river (in the southern coast) will produce channeling of the winds in the region.

The following sections will show the results of the application of TAPM model for a characteristic day of the synoptic situation of the two OSPs described in the previous section. The simulated day corresponds to day D (central day) of the group of three that describe every OSP, although simulations spanned over a 48-hour period, with day D – 1 used as spin-up of the model.

For each of the cases, figures shown represent the topography of Catalonia included in the inner domain of the simulation (2-km resolution), the 2-dimensional winds obtained with TAPM at the first vertical level (10 agl). For clarity we have only represented winds every four model cells

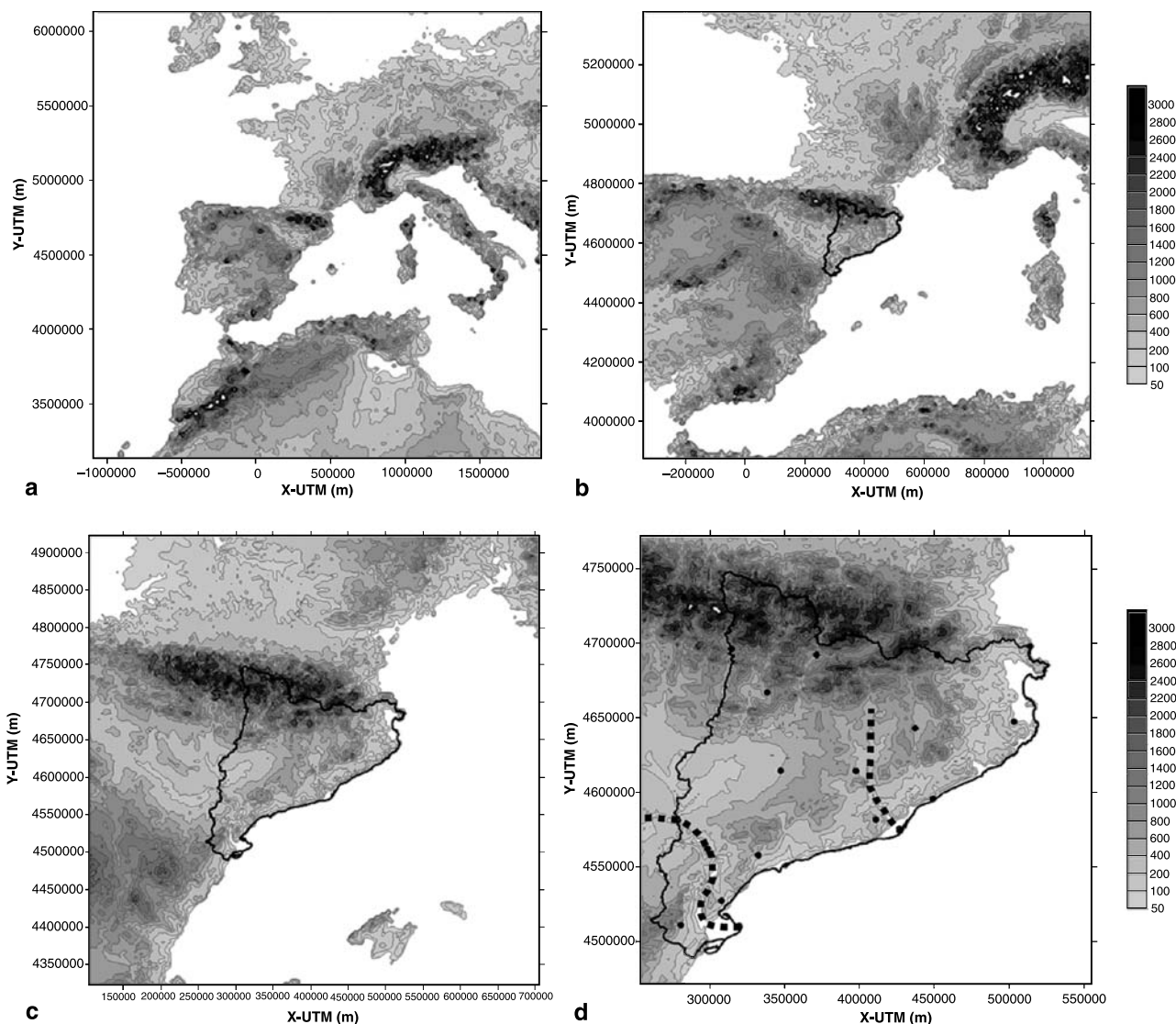


**Fig. 4.** Topography of the four nested domains used in the runs with the mesoscale model. From the top left corner to the bottom right corner, domains with 20, 10, 4 and 2 km resolution. The black line contours the region of Catalonia. In the 2-km resolution plot, the dashed lines indicate the position of the two main river valleys, and the dots show the location of the stations used for evaluation of the mesoscale model

(that is, every 8 km). We have only included results of the model at two different times of the day (daytime and nighttime regimes), to give an idea of the diurnal cycle associated with the mesoscale circulation.

Both simulations have been evaluated using wind and temperature data for 15 stations within the region of Catalonia. Comparisons have been performed between hourly 10-meter height measurements of winds and temperature acquired in the stations and values for those variables predicted by the model at the lowest vertical model at the nearest  $2 \times 2 \text{ km}^2$  cell containing

the station. Fig. 4d shows the location of the stations used in this analysis. Table 3 includes a summary of the statistics calculated for both simulations. Statistics have been calculated for temperature and for wind speed (module). The statistics calculated have been means, bias, standard deviations of observed (STD\_OBS) and predicted (STD\_MOD) values, square root mean squared error (RMSE) and the index of agreement (IOA). The IOA (Willmott, 1981) is a measure of how well predicted variations from the observed mean are represented and match the observations' departures from the observed

**Table 3.** Statistics at 10 m above the ground for TAPM simulations and measurements acquired at near-surface meteorological monitoring sites. Variables analyzed are: T (temperature), and Vel (wind velocity, module)

	MEAN_OBS	MEAN_MOD	STD_OBS	STD_MOD	RMSE	IOA
OSP6						
T	23.49	22.76	4.55	3.87	1.33	0.94
Vel	2.82	3.8	2.26	1.70	1.55	0.75
OSP5						
T	22.64	22.36	5.24	4.64	3.81	0.86
Vel	3.89	5.84	3.78	4.29	3.70	0.79

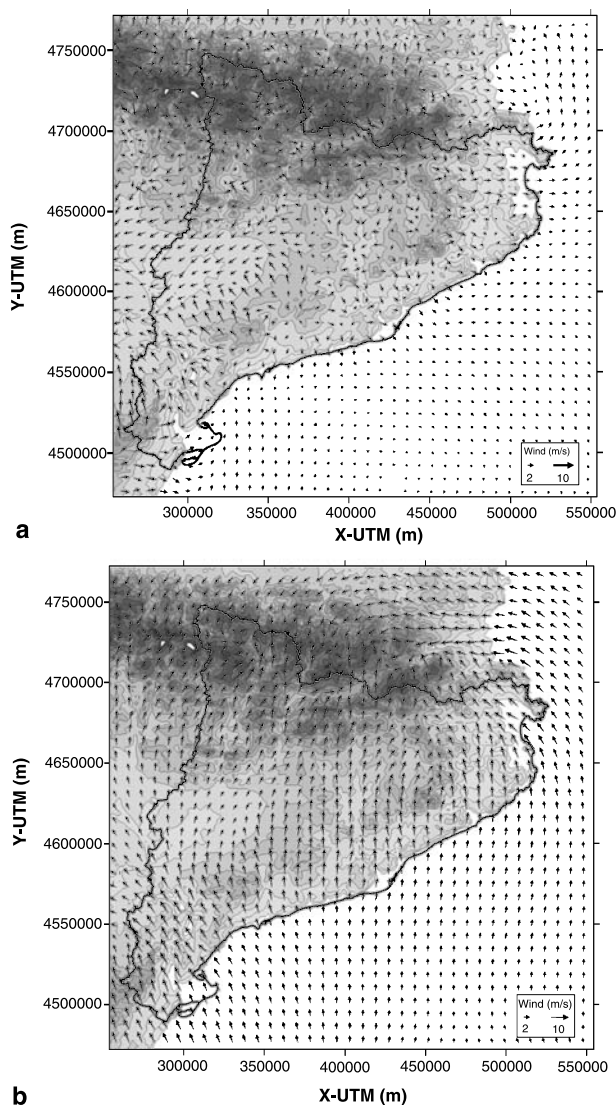
mean, with a value greater than about 0.50 considered to be good, as judged by several other published prognostic modeling studies (Hurley, 2000). An IOA equal to 1.0 would indicate a perfect agreement.

Results show that the set of stations analyzed had a large dispersion in the measurements. This can be seen in the large value of the standard deviation for the considered variables under the two situations analyzed. The large variability of the wind data along the modeled region and also along the daily cycle explain this fact. In general TAPM over predicts velocity and slightly under predicts temperature, although standard deviations are similar (and large) both in the measured and the modeled data. There are differences between the modeled and observed data, but in general RMSE values are lower than the standard deviation of the observations, indicating skill of the model. IOA are always higher than 0.75, and larger for temperature and for wind module than for wind.

Finally, and to complete the evaluation of the model, a qualitative comparison between modeled and observed values of winds has been included in the analyses of the two OSPs simulations described in the following sections. For several of the stations considered in the statistical analysis, we have represented time series of wind speed and direction, to evaluate the skill of the model to reproduce the daily cycle of this variable.

#### 4.1 Circulatory patterns under OSP6

Figure 5 includes modeled wind fields in the inner domain for the first vertical level. Winds show a clear daily cycle for this OSP, characterized by a very weak pressure gradient over the region. Indeed, wind speeds are very low during nighttime, indicating a weak synoptic forcing as stated

**Fig. 5.** Horizontal winds modeled with TAPM in the inner domain ( $2 \times 2 \text{ km}^2$ ) for July 10, 1999 corresponding to OSP6 at 00 UTC (a), and at 12 UTC (b)

in the description of this OSP. Nocturnal cooling induces downslope winds in the mountains (katabatic winds). The nighttime plot shows, in narrow

valleys such as those in the Pyrenees, convergences at the bottom of the valleys. During night-time winds are weak with a general land to sea direction near the coast, showing a land-breeze circulation due to radiative cooling of the ground.

After sunrise the rapid heating of the surface leads to sea-breeze formation. During the early hours the sea-breeze is only present within a strip of a few kilometers inland, and its direction is perpendicular to the coastline. Later on, the convective cell associated with the sea-breeze grows and penetrates further inland, increasing velocity. In fact, studies conducted also with TAPM in a region in the interior of Catalonia, have demonstrated the penetration of the sea-breeze front more than 100 km inland (Soriano et al, 2003). The model also reproduced the bearing of the sea-breeze direction during the afternoon as its

velocity increases. The increasing Coriolis effect produces a progressive clockwise turn of the winds from southeastern to southern components.

Heating of mountain slopes induces upslope winds (anabatic). In the coastal mountain ranges, that are aligned parallel to the coastline, these winds have the same direction as the sea-breeze, therefore enhancing the general sea-to-land flow. This fact also helps the penetration of the front inland, overriding the coastal mountains (see wind fields at 12 UTC included in Fig. 5). In the Pyrenees these upslope winds are formed at both sides of the mountain range, originating a convergence zone at the ridge of the mountain (topographic injections).

After sunset, when solar heating of the terrain terminates there is a period of transition until the nocturnal regime takes over. This transition period

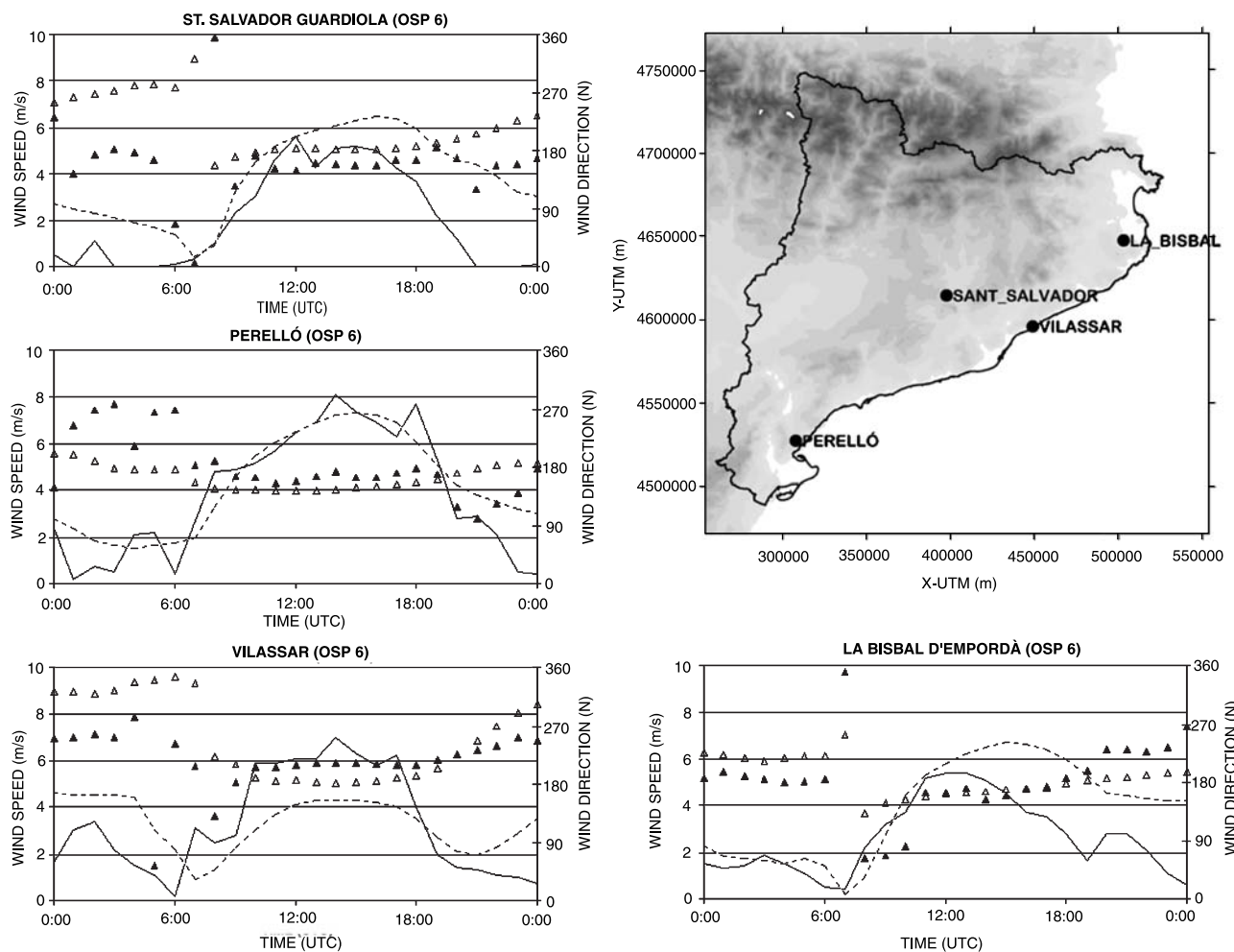


**Fig. 6.** Comparison of measured and predicted wind speed and directions for several stations (indicated in the right map) for OSP6 (July 10, 1999). Black triangles correspond to measured wind directions, empty triangles predicted wind direction, full line corresponds to measured wind speed and dashed line corresponds to predicted wind speed

is characterized by very weak winds and with very variable directions, lasting until the night cooling produces katabatic winds and nocturnal drainages.

Figure 6 shows comparison between modeled and predicted winds for July 10, 1999. Hourly data shows the important daily cycle of the wind under this synoptic situation. In general, for most of the stations winds are weak during nighttime and with rather erratic directions (this fact makes them difficult to predict with the model). During daytime, however, all of them show a rather steady direction which coincides with the establishment of the sea-breeze regime and higher wind speeds. The onset of this on-flow circulation is well reproduced by the model, and takes place sooner or later in the day depending on the position of the station and how close it is to the coastline.

With the mesoscale model we have simulated another day (July 24, 1999) that also had been classified by the objective synoptic analysis as belonging to OSP6. The wind field in Fig. 7 (corresponding to the daytime situation, at 12 UTC), shows similar circulatory patterns as those just described for July 10, 1999. For this day we can also see the penetration of the on-shore flow, and its bearing towards the South in the central coast. Statistics for the two cases gave similar results, with average velocity and standard deviation respectively of 4.20 m/s and 1.18 m/s for the first case and 4.22 m/s and 1.02 for the second case.

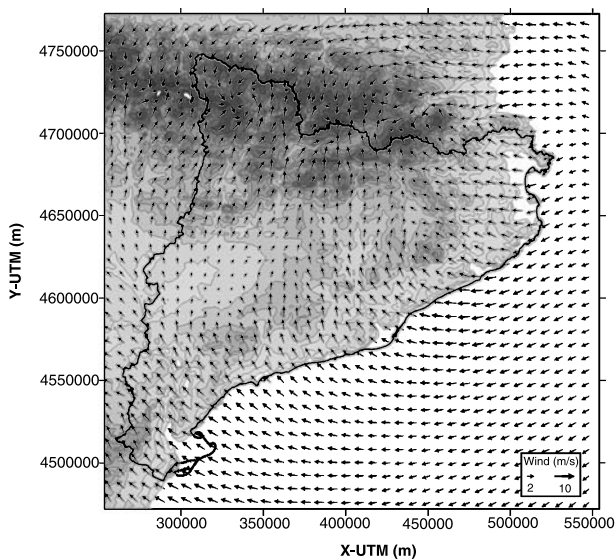


**Fig. 7.** Horizontal winds at 12 UTC modeled with TAPM in the inner domain ( $2 \times 2 \text{ km}^2$ ) for day July 24, 1999, also classified as corresponding to OSP6

#### 4.2 Circulatory patterns under OSP5

The synoptic situation under OSP5 is associated to a vigorous north-northwesterly flow. Under this large-scale forcing the diurnal cycle of the local winds (that usually is associated with the mesoscale part of the flow) is less evident that under OSP6 studied above.

This large-scale forcing is specially evident in the high-resolution simulation over Catalonia in the form of strong winds in its northern and southern limits. Figure 8 shows, for instance, how the presence of the Pyrenees acts as a barrier to the northerly winds and the flow accelerates in

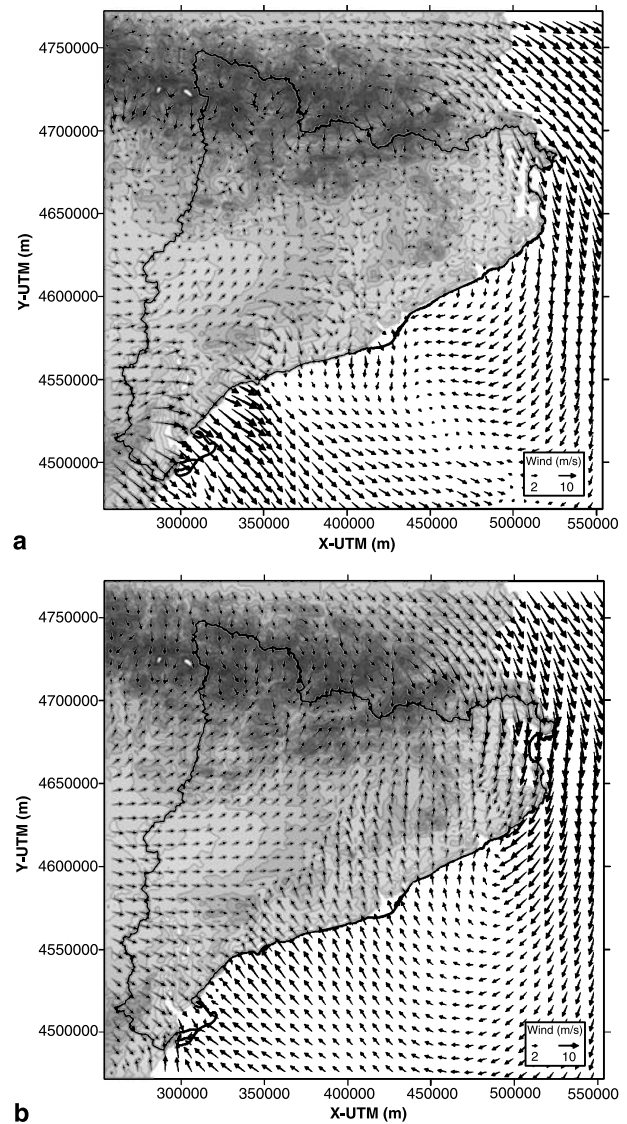


**Fig. 8.** Horizontal winds modeled with TAPM in the inner domain ( $2 \times 2 \text{ km}^2$ ) for day July 14, 1999 corresponding to OSP5 at 03 UTC (a) and at 15 UTC (b)

its exit towards the Mediterranean through the Gulf of Lyon. This fact produces the well known episodes of strong and constant winds named Mistral in the South of France or Tramontane in North Catalonia.

The northerly flow can also penetrate through the most western corner of the Pyrenees (its Cantabric end). The entrance of the flow is channeled through the Ebro river valley (evident in the result of the simulations over the third domain, not shown here), and produces extremely high winds at the end of the river valley and in its mouth at the Mediterranean Sea (winds locally known as *cierzo*). These winds are constantly present along the simulation period and show very little variation.

With sunrise, a typical on-shore sea-breeze circulation is established in the central coast of Catalonia. In this area the synoptic flow is not so

evident, and diurnal heating (remember we are studying a summer day) is strong enough to generate the mesoscalar circulation. The daytime wind field plot clearly shows the formation of a convergence line where the northwesterly flow associated with the synoptic forcing meets the sea-breeze on-shore front. In particular, at 15 UTC a convergence line can be seen in the north of Catalonia, with a NW–SE orientation, where Tramontane winds meet southerly sea-breeze winds. Another convergence line is formed in the central coast, with an orientation almost parallel to the coastline, where the general westerly flow meets the on-shore flow. This convergence line moves inland during the afternoon as the sea-breeze intensifies.

Finally, it should be noted that the entrance of the sea-breeze flow does not take place in the southern Catalan coast until the end of the

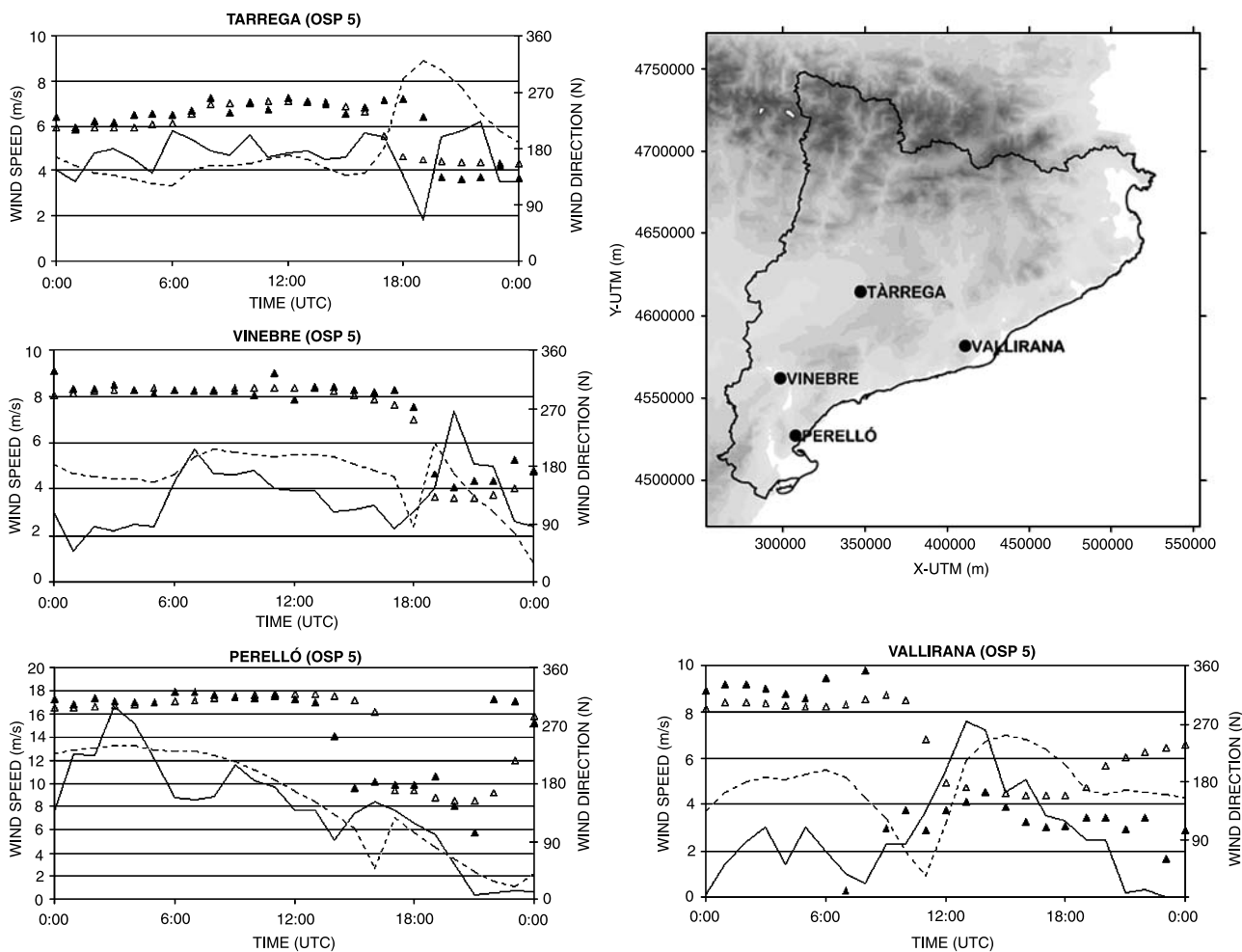


**Fig. 9.** Comparison of measured and predicted wind speed and directions for several stations (indicated in the right map) for OSP5 (July 14, 1999)

afternoon (see also Fig. 9 to confirm this point). The drainage in the Ebro valley is so strong due to the channeling of the synoptic flow that the sea-breeze front cannot penetrate inland until it reaches its maximum development, by late afternoon. Only then can an on-shore flow be observed in this region.

Figure 9 shows the comparison between modeled and predicted winds for July 14, 1999. The stations included in this daily-cycle analysis have a rather different behavior under this synoptic situation. In general, all of them show persistent westerly to northwesterly winds during nighttime, in agreement with the large-scale forcing. Agreement between modeled and predicted wind direction is very good at those hours. Daytime data show the onset of a weak sea-to-land circulation, which takes place sooner at stations located on the central Catalan coastline (Vallirana), while it can only be observed for very few hours and later in the afternoon at stations on the southern coast (Perelló and Vinebre). At stations located further in the interior of the region (such as Tàrraga) the sea-breeze front is not detected.

## 5. Conclusions

This work has shown how important it is to have a good knowledge of the mesoscale atmospheric circulatory patterns in regions with complex orography, given the significant horizontal variability of wind fields. Also, it has been shown how different these circulatory patterns can be under various synoptic forcings, resulting in very diverse local winds.

To help prove this point, we have carried out an objective classification of the synoptic processes, thereby obtaining large-scale situations, typical for the area studied, each having different frequencies of occurrence. We have run a high-resolution mesoscale model for a characteristic day of some of the situations, which has allowed us to describe the local atmospheric circulatory patterns in the region associated with the synoptic situation.

Simulations have confirmed the complex atmospheric circulatory patterns in the region, and the skillfulness of the mesoscale model to adapt the synoptic flow to local orographic features. The methodology has demonstrated the usefulness of the combined application of the classification of

the synoptic processes and the simulations with a mesoscale model to obtain a catalogue of regional wind patterns.

## Acknowledgements

The authors would like to thank the two reviewers (one of which was Ricardo M. Trigo, from the University of Lisbon, and who authorized the editor to reveal his identity) for their accurate review of the original manuscript, and for their useful comments and suggestions, which have definitely contributed to the improvement of this paper. Cecilia Soriano specifically acknowledges Jordi Cunillera, from the Catalan Meteorological Service (METEOCAT), for providing the surface data necessary for the validation of the simulations. She also thanks Bill Physick and Peter Hurley, from CSIRO Atmospheric Research, in Australia, for their assistance with TAPM and for providing the synoptic data for the model runs. Finally, part of this research has been undertaken in the frame of projects REN2001-2865-C02-01/CLI and REN2003-03436/CLI (Spanish Ministry of Science and Technology) and the “Grupo de Climatología” (2001SGR 00040, Catalan Government).

## References

- Bardossy A, Plate EJ (1992) Space-time model for daily rainfall using atmospheric circulation patterns. *Water Resources Res* 28: 1247–1259
- Capel Molina JJ (2000) El clima de la península Ibérica. Barcelona: Ariel
- Corte-Real J, Qian B, Xu H (1998) Regional climate change in Portugal precipitation variability associated with large-scale atmospheric circulation. *Int J Climatol* 18: 619–635
- Corte-Real J, Qian B, Xu H (1999) Circulation patterns, daily precipitation in Portugal and implications for climate change simulated by the second Hadley Centre GCM. *Clim Dyn* 15: 921–935
- Dünkeloh A, Jacobeit J (2003) Circulation dynamics of Mediterranean precipitation variability 1948–98. *Int J Climatol* 23: 1843–1866
- Esteban P, Jones PD, Martin-Vide J, Mases M (2005) Application of multivariate statistical techniques for the characterization of the surface circulation patterns related to heavy snowfalls in Andorra, Pyrenees. *Int J Climatol* 25: 319–329
- Fernández AJ, Díaz YA (in press) Catálogo de los procesos sinópticos en el archipiélago cubano. Cienfuegos: Centro Meteorológico Provincial, Imprenta GeoCuba, 170 pp
- Fernández AJ, Martín Vide J, Díaz YA, Mestre A (2003) Aplicación de los procesos sinópticos objetivos a la Península Ibérica en otoño. *Investigaciones Geográficas* 31: 37–65. Alicante: Universidad de Alicante
- Font Tullot I (1983) Climatología de España y Portugal. Madrid: Instituto Nacional de Meteorología
- Galán E (1989) Tipos de tiempo anticiclónicos invernales en la España peninsular y Baleares. *Ensayo metodológico*, Universidad Autónoma de Madrid (Phd thesis), 1405 pp

- Goodess CM, Jones PD (2002) Links between circulation and changes in the characteristics of Iberian rainfall. *Int J Climatol* 22: 1593–1615
- Goodess CM, Palutikof JP (1998) Development of daily rainfall scenarios for southeast Spain using a circulation-type approach to downscaling. *Int J Climatol* 10: 1051–1083
- Hart T (1998) Upgrade of the global analysis and prediction (GASP) system. Bureau of Meteorology Operations Bulletin No. 45
- Hurley P (2002) The Air Pollution Model (TAPM) Version 2. Part 1: Technical description. CSIRO Atmospheric Research Technical Paper No. 55. See [www.dar.csiro.au/TAPM](http://www.dar.csiro.au/TAPM)
- Hurley PJ, Blockley A, Rayner K (2001) Verification of a prognostic meteorological and air pollution model for year-long predictions in the Kwinana: industrial region of Western Australia. *Atmos Environ* 33: 1871–1880
- Jenkinson AF, Collison BP (1977) An initial climatology of gales over the North Sea. Synoptic Climatology Branch Memo. 62, Meteorological Office, Bracknell
- Kalnay E, Kanamitsu M, Kistler R, Collins W, Deaven D, Gandin L, Iredell M, Saha S, White G, Woollen J, Zhu Y, Leetmaa A, Reynolds B, Chelliah M, Ebisuzaki W, Higgins W, Janowiak J, Mo KC, Ropelewski C, Wang J, Jenne R, Joseph D (1996) The NCEP/NCAR 40-Year Reanalysis Project. *Bull Am Meteorol Soc* 77(3): 437–471
- Linés A (1981) Perturbaciones típicas que afectan a la península Ibérica y precipitaciones asociadas. Madrid: Instituto Nacional de Meteorología
- Martín-Vide J (1991) Mapas del tiempo: fundamentos, interpretación e imágenes de satélite. Barcelona: Oikos-tau
- Martín-Vide J (2002) Aplicación de la clasificación sinóptica automática de Jenkinson y Collison a días de precipitación torrencial en el este de España. In: *La información climática como herramienta de gestión ambiental* (Cuadrat, Vicente y Saz, eds), pp 123–127. Universidad de Zaragoza y Asociación de Geógrafos Españoles.
- Millán M, Salvador R, Mantilla E (1997) Photooxidant dynamics in the Mediterranean basin in summer: results from European research projects. *J Geophys Res* 102: 8811–8823
- Puri K, Dietachmayer G, Mills G, Davidson N, Bowen R, Logan L (1998) The BMRC Limited Area Prediction System, LAPS. *Aust Meteorol Mag* 47: 203–223
- Rasilla D (2003) Aplicación de un método de clasificación sinóptica a la Península Ibérica. *Investigaciones Geográficas* 30: 27–45
- Romero R, Ramis C, Guijarro JA (1999a) Daily rainfall patterns in the Spanish Mediterranean area: an objective classification. *Int J Climatol* 19: 95–112
- Romero R, Sumner G, Ramis C, Genovés A (1999b) A classification of the atmospheric circulation patterns producing significant daily rainfall in the Spanish Mediterranean area. *Int J Climatol* 19: 765–785
- Shubert S (1994) A weather generator based on the European Grosserwetterlagen. *Climate Res* 4: 191–202
- Soriano C, Soler RM, Pino D, Alarcón M, Physick B, Hurley P (2003) Modeling different meteorological situations in Catalunya, Spain, with MM5 and TAPM mesoscale models: a comparative study. *Int J Environ Pollut* 20: 1–6, 256–268
- Spellman G (2000) The application of an objective weather-typing system to the Iberia peninsula. *Weather* 55: 375–385
- Stull RB (1988) An introduction to boundary layer meteorology. Dordrecht: Kluwer Academic Publishers, 666 pp
- Trigo RM, DaCamara CC (2000) Circulation weather types and their impact on the precipitation regime in Portugal. *Int J Climatol* 20: 1559–1581
- Willmott CJ (1981) On the validation of models. *Phys Geogr* 2: 184–194
- Zhang X, Wang XL, Corte-Real J (1997) On the relationships between daily circulation patterns and precipitation in Portugal. *J Geophys Res* 102(D12): 13495–13507

Corresponding author's address: Dr. Cecilia Soriano, Universidad Politècnica de Catalunya (UPC-ETSEIB), Departamento de Matemàtica Aplicada I, Av. Diagonal 647, 08028 Barcelona, Spain (E-mail: [cecilia.soriano@upc.edu](mailto:cecilia.soriano@upc.edu))